Energy Budget of a Mediterranean system affecting the weather of Saudi Arabia

A. K AL-Khalaf

Department of Meteorology, Faculty of Meteorology, Environment, and Arid Land Agriculture, King Abdulaziz University, Jeddah, Saudi Arabia.

ABSTRACT

Analysis of the kinetic energy budget for a developing winter-type cyclone is presented. This case represents a middle latitude cyclone that is developed significantly north of the Mediterranean Sea. The development occurred as cold fresh air is advected to the rear of the system. The role of the polar and subtropical jets is discussed. It found that horizontal flux convergence constitutes the major energy source and is the main cause for maintaining the strength of the upper tropospheric jet maxima. Generation of kinetic energy via cross-counter flow is a persistent sink at the most days. Dissipation of kinetic energy, computed as a residual, has local maxima both in the lower troposphere and near the jet stream level. Spatial fields of the energy terms show that the most intense energy processes occur associated with deep cyclogenesis. The vertical transfer of kinetic energy acts as s source of kinetic energy to middle troposphere and lower stratosphere.

1. Introduction

Changes in atmospheric energy are associated with meteorological phenomena of all scales. An understanding of the energy processes of various scales of motion should help to explain and forecast many weather events that are not adequately understood. It is apparent from numerous investigations (e.g., Smith, 1973; Ward and Smith, 1976; Chen et al.,1978; Fuelberg and Scoggins, 1978: Abdel Wahab and Abdel Basset, 2000; Pant, 2005 and Tsing and Yen, 2004) that kinetic energy sources and sinks show considerable spatial variation within individual synoptic-scale waves. Such inhomogeneities are especially prominent in the presence of a strong westerly jet core, where both transport and baroclinic conversion processes are maximized. In addition, highly variable energy fields are observed in the presence of intense prefrontal convection, which is often embedded within these jet flows. Although strong jet streams and convective regions are known to be energetically active, understanding of the processes within such flow regimes remains incomplete. This is primarily

due to the fact that these regimes are strongly influenced by processes that are subgrid-scale with respect to the current upper air synoptic network.

Most of the works in energy diagnosis at the mid-latitude system were conducted in terms of case studies of individual cyclones. A partial list of significant contributions may include works by Fuelberg and Jedlovec (1982), Yousef (1998) and Abdel Wahab and Abdel Basset (2000). It has been long recognized that the eddy disturbance assume a dominant role in the transfer and transformation of energy in the middle latitude. (e.g Wiin-Nielsen 1968; Michaelides 1992; Michaelides *et al.* 1996; H. Abdel Basset 2001; Silas Chr Michaelides, 2006). Energetics study on climatological features of the Asian Summer Monsoon was made by Mohanty et al. (2005).

The purpose of the present study is to discuss and analyze the kinetic energy budget during the life cycle of the cyclone over a limited area during 18 to 26 January 2005. The system represents a middle latitude cyclone that developed significantly northwest of the Europe mainly due to baroclinic effects in association with strong activity of the polar and subtropical jets. In the following sections, we discussed the kinetic energy equation, the data sources and method of analysis, the synoptic situation for the cyclone and finally the kinetic energy budget in association with the life cycle of the cyclone.

2. Theoretical considerations

The kinetic energy equation

The kinetic energy equation given by Smith (1969) is applicable to hydrostatic, open systems. The equation in isobaric coordinates is

$$\frac{\partial K}{\partial t} \equiv \frac{1}{sg} \int_0^{P_0}\int_S \frac{\partial k}{\partial t} dsdP = -\frac{1}{sg} \int_0^{P_0}\int_S \nabla \cdot (Vk)dsdP - \frac{1}{sg} \int_0^{P_0}\int_S \frac{\partial(\omega k)}{\partial P} dsdP$$

$$-\frac{1}{sg} \int_0^{P_0}\int_S V \cdot \nabla \phi \, dsdP - D(k), \qquad (1)$$

Where S is the area of computational domain, g is the acceleration due to gravity and P_o is the surface pressure. On the right-hand side of (1), the first and second terms are the horizontal and vertical flux divergence of kinetic energy, the third term is the generation of kinetic energy due to the cross-contour flow and the last term D (k) is commonly called the "dissipation" term.

3. Data and computation

a- Input data

The data used in this study have been taken from the archives of the European Center for Medium Range Forecasting (ECMRF). It consist of the horizontal wind components (u-eastward, v-northward), the temperature (T) and the geopotential height (z) on regular latitude-longitude grid points with resolution of 2.5^{o} x 2.5^{o} . The available data is at 0000 and 1200 GMT during the period 18 to 26 January 2005 for isobaric levels 1000, 850, 700, 500, 300, 200 and 100 hPa. Figure 1 show the domain of the study which extends from 10° to 70° N and from 10° W to 60° E. The inner domain that is used in our calculation for the present study changes with time to enclose the cyclone during its life cycle (see Figure 2).

b- Analytical procedures

The vertical wind component in the p-coordinate system, namely $\omega=dP/dt$,is estimated using the kinematic method. However, due to errors in horizontal divergence estimates, accumulation of error in ω occurs away from the bottom of the atmosphere. To remove this bias a pressure-weighted correction for ω was adopted following O'Brien (1970). This technique was employed calculate grid point values of ω at all isobaric levels and at the midpoint of each sublayer. At the bottom and the top of the atmosphere ω was initially set to zero. The energy variables in equation 1 are calculated at 1200 GMT. Therefore, time derivatives evaluated by central differences spanning 48 h give a reasonable indication of the time variation of kinetic energy Centered finite differences were used to compute horizontal derivatives and all vertical derivatives except those at the 1000 and 100 mb, where non-centered differences were employed. Finally, the dissipation term is evaluated as a residual in (Kung, 1966). Holopainen,(1973) warns of the risk of attaching physical significance to the sign or magnitude of residual terms, but concedes that application of the residual technique may be meaningful in data-rich areas.

4. Synoptic discussion

A common case of winter cyclogenesis over the Mediterranean is considered in the present study. Its period extended from 18 to 26 January 2005. Based on 1000 hPa and 500 hPa charts the life cycle of this cyclone can be divided into two periods. The first period

(growth period) is from 18 to 23 January while the second period (decay period) is from 24 to 26 January. 1000 hPa and 500 hPa charts at 1200 GMT on each day are shown in Figurs 1 and 2 respectively. 1000 hPa charts depict contours of height with 20 geopotential meter (GPM) increment while upper air charts (500 hPa) contain contours of height with 40 GPM increment. The isotherms in the charts of the two levels are analyzed with $5^{o}C$ increment. The cyclone of special interest first appeared as an extension of the traveling depression north west of Europe at 18 January. A cut-off low is formed at 19 January and a well-defined cyclonic depression become clear over south west of Italy. At 19 January a strong thermal gradient lies along the northern Italy and middle of Europe. In this highly baroclinic zone the surface storm undergoes strong intensification.

The evolution of the lee cyclogenesis was consistent at least in the second and third days, with the schematic processes outlined in Buzzi and Tibalidi (1978). The interaction of the cold front with the Alps produced the initial disturbances which then grow as a baroclinic disturbance.

During the next 24 hours, the the center of the low propagates slowly to the southeastward and the geopotential height at the center reaches to 20GPM (Fig. 1c). A corresponding cut off low at 500 hPa becomes over north libya with center of 5400 GPM. On 21 January a strong development occurs at the surface and at the upper air, where the surface cyclone moved east ward and becomes continued (joints) with the main cyclone (its center at $55^{o}N$, $25^{o}E$). Also the inverted v-shap trough of the Sudan low oscillate north ward to the north of the red sea and in the upper air (500 hPa) the cut of low also moved east ward to a point just north east of Egypt. At 1200 GMT 22 January (the rainy day), a strong interaction occurs between the trough that extended from the tropical region and that extended from middle latitude region, and the two cyclones becomes joints with other. The most interesting features is that there is north ward strong warm advection from the tropical region associated with the air flow around the Sudan low and a south wad strong cold advection. The interaction between these two air masses causing a strong instability over the east of Mediterranean and at the west of Saudi Arabia. By 1200 GMT January, the trough of Sudan low moved south west ward with the trough of the midllatitude low moved east ward to centered over Iran. During the next two days (25 and 26 January) the depression started filling and its central pressure increased gradually. On the other hand the high pressure over Atlantic is extended with a major ridge that joints the Siberian high on 22 January, Fig.1d. In other

wards no more cold advection is permitted from the to the cyclone. While the Siberian high pressure propagate westward the horizontal extension of the cyclone decrease and moved slowly eastward, and it become stationary vortex rotating above the north east of Mediterranean. Finally the cyclone was drifted slowly north-eastward and was out of the computational domain by 25 January.

The behavior of the subtropical and polar jets

It is known that the subtropical (polar) jet has its maximum speed around 200 hPa (300 hPa). So, we display the 300 and 200 hPa isotach fields in the following discussion to show the behavior of the polar and subtropical jets during the development of our case study. Figs. 3 and 4 display the isotach (wind speed) at 300 and 200 hPa from 18 to 25 January 2005. They show the behavior of the subtropical and polar jets at 200 and 300 hPa levels during the life cycle of our cyclone. On 18 January 2005 (Fig. 3a) the wind direction over north Africa is zonal and the maximum speed of the subtropical jet is 65 m/s and is located over northeast of Africa (over Libya, Egypt and north Red sea), its value at 200 hPa is greater than 75 m/s. The polar jet extended from northwest England to southeast Spain and north of Italy with a maximum wind greater than 75 m/s at 300 hPa, its extension at 200 hPa has a maximum wind greater than 65 m/s. On 19 January 2005, the subtropical jet moves slightly to eastward and its maximum canter becomes greater than 65 m/s at 300 and 200 hPa and was located over Saudi Arabia. While the polar jet is shifted eastward and moved south eastward to amalgamate with the subtropical jet and its maximum value becomes greater than 70 m/s at 300 and more than 60 m/s at 200 hPa. On 20 January, the subtropical jet was shifted to the southeast. The front of the polar jet reaches north of Algeria and its jet maximum wind value is greater than 75 m/s at 300 and 200 hPa. The subtropical jet weakened at 300 hPa and became stronger at 200 hPa (>70 m/s) and moved eastward. The amalgamation between the two jets continuous also at 21 January. Beginning with the day of 22 up to 25 January the polar jet weakened at 200 hPa and the amalgamation with the subtropical jet disappears. On 24 and 25 January the polar jet extended from north Europe to northwest Africa with a maximum wind greater than 65 m/s at 300 hPa. During the last three days, we notice that the subtropical jet is moved westward and were almost back to the normal distribution in both speed and direction.

5. Analysis of total kinetic energy budget

5.1 Kinetic energy time development

The energy budget in terms of the Eulerian kinetic energy equation 1 is evaluated in a domain which encloses the cyclone during its life cycle. The area mean energy variables, integrated from 1000 to 100 hPa at 1200GMT are shown in table 1. Note that the vertical flux divergence was integrated to zero because of the solid boundary condition on ω, therefore is not presented in the table.

The kinetic energy K increase during the growth period reaches a maximum at 22 January 2005 and decreases gradually at the decay period. The local variation of kinetic energy $\partial k/\partial t$ positive most of the growth period of the cyclone except at 22 and 23 January when the cyclone tend to decay. The growth period is affected not only by the persistent of the upper troposphere subtropical jet but also by the entrance of strong polar jet in the areas of the computational domain (Figs. 3 and 4), therefore the kinetic energy increased.

Generation of kinetic energy is a prominent sink of energy during the first three days of the growth and decay periods. It acts as a source of kinetic energy at 21, 22 and 26 January. The magnitude of this term is evidence widespread and persistent imbalance in the mass and wind fields, the negative values of the generation term on average indicate that the cross contour flow is down gradient in the vicinity of the cyclone. The maximum destruction of kinetic energy by this term occurs at 1200 GMT 19 January, while the maximum generation of kinetic energy occurs at 1200 GMT 22 January.

The major source of kinetic energy is due to the horizontal flux convergence (-∇. KV). This term acted as a persistence source of energy for the all period of the cyclone except at 22 January. The greatest values of this term occur at the first day of the growth period and the last day of the decay period. The decay period of the cyclone is affected by the entrance of the strong subtropical jet area into the areas of the computational region, therefore the kinetic energy increase. The horizontal flux convergence is positive at every time step in this period and so acts as a source of energy.

Dissipation of kinetic energy from grid to subgrid scale is an important process during the life cycle of our cyclone. The results in table 1 reveal that a net transfer of energy from subgrid to grid scales (D (k) < 0) is most pronounced during the growth and decay period except at 19 and 20 January. Considerable positive values of the dissipation term represent

subgrid-scale to grid scale interaction are an energy source for the region at 19 and 20 January.

Table 1. Kinetic energy budget (1000 to 100 hPa). Units are Wm^{-2} except for energy content which are 10^{-5} Jm^{-2}

Date / time	K	$\partial K/\partial T$	$- V. \nabla\Phi$	$- \nabla. KV$	D (K)	$- V. \nabla\Phi + D (K)$
Growth period						
18 – 1 / 12	4.4	1.48	-4.91	10.5	-4.1	-9.01
19 – 1 / 12	5.72	0.93	-9.47	2.88	7.52	-1.95
20 – 1 / 12	7.08	0.37	-3.36	0.2	3.53	0.17
21 – 1 / 12	8.43	0.82	2.07	0.35	-1.61	0.47
22 – 1 / 12	10.13	-0.14	6.44	-3.7	-2.88	3.56
23 – 1 / 12	9.13	-1.06	-0.88	0.2	-0.37	-1.25
Decay period						
24 – 1 / 12	6.94	-0.43	-1.19	1.46	-0.69	-1.88
25 – 1 / 12	6.96	0.21	-1.99	5.25	-3.05	-5.04
26 – 1 / 12	7.3	0.47	2.81	11.88	-14.22	-11.41
Time mean	7.34	0.35	-1.16	3.22	-1.76	-3.32

5.2 Time-height variations of budget quantities

Energetic processes in relation to the cyclogenesis region need further examination and were analyzed by means of vertical- time cross sections as represented in figure 5.

The major contribution to kinetic energy comes from a persistent upper tropospheric jet stream activity throughout the period of study. The most of this energy occurred above 400 hPa in association with the strong jet stream. The maximum value occurred during the growth period, this can be noticed clearly on 22 and 23 January. The local derivative term indicates that the kinetic energy increase at all levels especially above 300 hPa in the first four days. With the beginning of 21 January the local variation of kinetic energy decrease at the lower levels (below 700 hPa) and at all levels on 22 and 23 January. The maximum decreasing of kinetic energy occurs at 22, 23 and 24 January above 500 hPa. Below 700 hPa at 24 and 25 and at all levels of 26 January another increase of kinetic energy occurs.

The term, $-\partial (\omega K) / \partial P$, indicate the vertical transport of kinetic energy, positive values indicating downward transport. Downward transport of kinetic energy is found for the first

three days in the growth period in the layer 850- 300 hPa. Above 300 hPa for the first three days in the growth period and below 300 hPa at 21 and 22 January and also below 200 hPa the vertical flux is negative which indicate that the transport of kinetic energy aloft by the upward vertical motion. This vertical transport acts as a source of energy to the upper troposphere in 21 and 22 January and to the stratosphere in 23 and 24 January. In 23 January and below 200 hPa this vertical transport acts as a source of energy to the middle and lower troposphere. However, the magnitude of the vertical flux term is relatively small with respect to the other terms.

The horizontal flux convergence had a positive sign during the first two days reached its maximum between 500- 200 hPa at the first day. A large amount of energy is transported out of the area by horizontal flux convergence (-∇ . KV <0) above 300 hPa specially near the level of the jet at 20, 21 and 22 January. Below 500 hPa in 21, 22 and 23, although the contribution of this term still small it may be considered as a sink of energy. The horizontal flux cpnvergence acts as a source of energy between 500- 300 hPa throughout the life cycle of our cyclone and also at the all levels for the last three days. The maximum import of kinetic energy into the region occurred at 200 hPa in 26 January.

The life cycle of our cyclone is apparent in the generation term (-V.$\nabla\Phi$). in the first three days of the growth period the major energy sink is the intense conversion of kinetic to potential energy by the generation term which reaches its maximum negative at 1200 GMT 19 January specially at 300 hPa. At 21 and 22 January the generation of kinetic energy is a prominent source of energy above 850 hPa while it acts as a sink of energy below 850 hPa throughout the period of our case except at 25 and 26 January. Weak generation of kinetic energy occurs at the decay period between 850- 500 hPa and at 200 hPa for 24 and 25 January. This term acts as energy sink at 300 and 100 hPa in 23, 24 and 25 January.

Dissipation of kinetic energy from grid to subgrid scales is an important process during the first day of our case. Positive dissipation term is suggesting a transfer of energy from subgrid to grid scale of motion as an important source of energy during 19 and 20 January. So, the large amount of energy is imported to the area by dissipation that acts as a source of energy at all levels with maxim near the level of the jet. The maximum positive dissipation values occur at 200 hPa on the second day (19 January). This term acts as a sink of energy above 500 hPa in 21, 22 and 23 January and above 850 hPa for the decay period. The maximum negative dissipation values occur at 200 hPa in the last day of our case. Positive

values of this term have been reported by numerous other investigators (e.g., Ward and smith, 1976; Chen and Bosart, 1977; and Tusi and Kung, 1977).

5.3 Horizontal distribution of budget quantities

The relationships between the evolving synoptic features and the ensemble cyclogenesis are now examined by considering the spatial distribution of budget terms. All quantities are 1000 to 100 hPa integrals except for the kinetic energy content, which is restricted to the 200-500 hPa jet stream layer.

Fields of kinetic energy content and local change are presented in figures 6 and 7. During the first day two centers of maximum values of kinetic energy located on the northwest corner and south of the Mediterranean sea and continues to propagate eastward (Fig. 6). The first center ($> 70 \times 10^4$ J m^{-2}) which is associated with the polar jet stream occurs over the north west of our domain (over England) while the second center ($>30 \times 10^4$ J m^{-2}) is associated with the subtropical jet and is located over the south part of Mediterranean (over the north of Libya). On the second day (19 January) the first center was shifted southeastward and its maximum weakened to about 50×10^4 J m^{-2} and it become located over the west of Mediterranean, while the second one is shifted northward and increased to about 65×10^4 J m^{-2}. This day represent the maximum amalgamation between the polar and subtropical jets. On day 20 January (where the amalgamation between the tow jets weakened), the first center is waked and moved more to southeastward and was located over Tunis and its extension became small. The second center increased and to about 85×10^4 J m^{-2} and becomes over south Libya. On 21 January, after the amalgamation of both jet, the polar jet disappear and the maximum values of kinetic energy associated with the subtropical jet increase to more than 90×10^4 J m^{-2}. On 22 January, the subtropical jet is shifted eastward and its core located over middle of Saudi Arabia. The maximum values of kinetic energy associated with the subtropical jet increase to more than 95×10^4 J m^{-2}. On 23 January, the subtropical jet is shifted westward and its core located over east of Mediterranean and the values of kinetic energy associated with it decrease to 60×10^4 J m^{-2}. On the last two days (24 and 25 January), where the subtropical jet is almost back to normal distribution in both speed and direction, its associated center of kinetic energy was weakened and moved westward.

The $\partial k/\partial t$ reflects the progression and reorientation of the kinetic energy fields. During the period of most active cyclogenesis (the growth period) the larger $\partial k/\partial t$ is located between the geometric centers of cyclogenesis. Propagation of the subtropical and polar jets is reflected in the $\partial k/\partial t$ maximums. Increase in kinetic energy greater than 7 Wm^{-2} occurred west of the storms (Fig. 7a). On 19 January the center of positive $\partial k/\partial t$ west of the cyclone is shifted eastward. The most pronounced variation on 20 January was the decrease in energy associated with the exit of the polar jet. Also, in 20 January two centers of pronounced increase of kinetic energy appears, the first one associated with the core area of the subtropical jet and located over north Egypt and east of Mediterranean, the second one associated with the polar jet and located over north Italy. The value of $\partial k/\partial t$ in the middle of the two centers reached 7 Wm^{-2}. with the movement of the two jets eastward the first center was shifted northeast ward and located over north east of Saudi Arabia with $\partial k/\partial t$ greater than 9 Wm^{-2}, while the second center moved southwest ward south of Italy. The area of negative $\partial k/\partial t$ is also shifted eastward. On 22 January (Figure 7e), the first center of $\partial k/\partial t$ becomes over Saudi Arabia and Red sea with pronounced decrease of it positive values, while the second center moved eastward and located over the center of Mediterranean with increase of its values (7 Wm^{-2}). The area of negative values of $\partial k/\partial t$ increased and occupied the most of our domain of calculation. On 23 January, the domain of our calculation is divided into two areas, the first one of negative values of $\partial k/\partial t$ occurs east of the domain and is affected by the weakness of the subtropical jet, while the second area are located over north Africa, Mediterranean and south east of Europe. On 24 and 25 January (Figures 7g and 7h), the filed of $\partial k/\partial t$ reflects the propagation and movement of the subtropical jet were it moved eastward and was almost back to the normal distribution in both speed and direction.

Kinetic energy generation fields (Figs. 8) are dominated by a broad region of strong conversion of kinetic to potential energy that propagates slowly eastward. The fields of $-V.\nabla\phi$ had two regions, the first which is located in the left side of the upper air trough (see Fig.2) has negative sign, while the second which is located in the right side of upper air trough is positive. The magnitude of the negative values is greater than of the positive ones, so the destruction of kinetic energy is much greater than the generation. The maximum conversion of kinetic to potential energy occurs at the second day of the growth period, where maximum negative values greater than –40 W m^{-2} are located north and west Europe at 19 January,

while maximum positive value greater than 10 W m^{-2} are east of our domain at the first three days. Maximum positive values greater than 15 W m^{-2} are located northeast Saudi Arabia at 22 January, while the largest region of negative values appears at 24 and 25 January. The maximum conversion of kinetic energy to potential energy occurs at the last day of the decay period (26 January).

The horizontal flux convergence is the major budget sources as indicated by the statistics in table 1. Figure 9 show that the maximum centers of horizontal flux convergence occur just east of the kinetic energy content and jet maximum. It is interesting to note that the positive centers of -∇.kV at the northwest of our domain (above west of Europe) were found associated with the centers of maximum energy and with centers of maximum wind of the polar jet throughout the first two days (18- 19 January). Also we notice on 20 January that corresponding to the centers of maximum kinetic energy and the subtropical jet above northeast of Africa there are two centers of -∇.kV. The first was positive and located above Egypt and east of Mediterranean while the second was located west of the first. This two centers oscillate (west to east or east to west) and intensify in association with the oscillation and intensification of the subtropical jet throughout the period of our cyclone. In general the horizontal flux convergence maxims are positioned just downstream from the jet maxim in the regions of diffluent flow. As shown by Uccllini and Johnson (1979) supergeostrophic flow a head of a jet maximum may act through its circulation to reinforce the low-level jet, thus enhancing the differential moisture and thermal transport will maintain favorable conditions for development deep cyclogenesis. On 20 January, the first center which indicate a major source of kinetic energy extend northeast ward with maximum values greater than 20 Wm^{-2} are located over northeast of Egypt. The positive values of this center increases during the following two days (21 and 22 January). There is also area of positive -∇.kV located over the northwest of our domain of calculation. The positive values of this area increases at 21 January and decreases in 22 January, it nearly disappeared in the last days. On 22 January the area of negative values increased and extended northeast ward. The magnitude of the negative values in this days are greater than those of positive values, so, in average the horizontal flux convergence acts as an energy sink. With the west ward movement of our cyclone the centers of negative and positive values moved west ward with high decrease of the magnitude of negative values (Figure 9f). on 24 and 25 January, the cyclone also moved slowly east ward

and the subtropical jet also moved eastward to back to its normal situation. This can be shown from the fileds of $-\nabla.kV$ in figures 9g and 9h.

The dissipation fields (Figs. 10) contain substantial regions of positive values, indicating subgrid- scale kinetic energy sources. Although the dissipation term is subject to computational uncertainty, positive $D(k)$ values appear to be related to the presence of cyclogenesis. In our case a substantial portion of the cyclogenesis develops within regions of positive values, taking consideration those positive values weakened during the decay period. In this case of study, each dissipation field divided into two regions the first contained positive values and the second contained negative values. The regions containing positive values were located in the left side of our domain and oscillate eastward especially during the growth period, while the negative values regions was located in the right side. Strong association is observed between the dissipation region of positive values and the region of negative values of $-\nabla.kV$, and also between the dissipation regions of negative values with the regions of positive values of $-\nabla.kV$. The association can be seen by comparing the distributions of $D(k)$ in figure 10 to those in figure 9 of $-\nabla.kV$. On 19 and 20 January the magnitude of the positive values is much greater than the magnitude of the negative values this indicates that the transfer of energy from the subgrid to the grid scale may have provided an important source of energy, the inverse is true throughout the other days of this case (Figure 10).

6. Conclusion

Kinetic energy budget of a Mediterranean cyclonic system have been studied in terms of time area- average statistics, spatial distributions of vertical integrals and time- height cross sections. The most significant findings are as follows:

1- The major contribution to kinetic energy comes from a persistent upper tropospheric jet stream activity throughout the period of the cyclone. Most of this energy occurred above 400 hPa in association with the strong jet stream.

2- The horizontal flux convergence behaves as a major energy source during the life cycle of our cyclone, while generation of kinetic energy via cross- contour flow acts as a persistent sink except only at the two days of maximum cyclogenesis in the growth period.

3- Subgrid-scale sources of kinetic energy provide a substantial energy loss throughout the life cycle of the cyclone except at the two days of maximum cyclogenesis. Generally, dissipation of kinetic energy nearly balancing the generation term, this balance of

source and sink terms is basically similar with maximum generation and dissipation in the lower troposphere and at the jet stream level.

4- Temporal variations in the generation term, flux convergence and dissipation terms of kinetic energy budget are related to the life cycles of the cyclone where maximum energy conversion and transport occur near the time of maximum storm intensity while smaller values are observed during the development and decay stages.

5- Spatial fields of the energy terms show that the most intense energy processes occur associated with deep cyclogenesis.

6- The vertical transfer of kinetic energy, $-\partial(\omega K)/\partial P$, acts as s source of kinetic energy to middle troposphere and lower stratosphere.

References

Abdel Basset. H., 2001: Energy conversion of a desert depression. Meteorol. Atmos. Phys. Meteorol. Atmos. Phys. 76, 203- 222.

Abdel wahab. M and H. Abdel Basset, 2000: The effect of moisture on the kinetic energy of a Mediterranean cyclone. Theor. Appl. Climatol. 65, 17-36.

Abdel wahab. M and H. Abdel Basset, 2000: Energy Exchanges for Mediterranean Weather Systems. Meteorol. Atmos. Phys. 73, 1- 23.

Buzzi, A. and S. Tibaldi, 1978: Cyclogenesis in the lee of the Alps: a case study. Q. J. R. Meteorol. Soc. 104, 271- 287. Red River Vally tornado outbreak (AVESESAME I). Mon. Wea. Rev., 110, 2005- 2024.

Chen, T. C., and L. F. Bosart, 1977: Quasi- Lagrangian kinetic energy budgets of comosite cyclone- anticyclone couplets. J. Atmos. Sci., 34, 452- 464.

Chen, J.C., P. Alpert and T.W. Schlatter, 1978: The effects of divergent and nondivergent winds on the kinetic energy budget of a midlatitude cyclone: A case study. Mon. Wea. Rev., 106, 458-468.

Fuelberg, H.E., and G.J. Jedlovec, 1982: A subsynoptic-scale kientic energy analysis of the Red River Valley tornado outbreak (AVESESAME I). Mon. Wea. Rev., 110, 2005-2024.

Fuelberg, H.E., and J.R. Scoggins, 1978: Kinetic energy budgets during the life cycle of intense convective activity. Mon. Wea. Rev., 106, 637-653.

Holopainen, E., 1973: An attempt to determine the effects of turbulent friction in the upper troposphere from the balance requirements of the large-scale flow: A frustrating experiment. Geophysica., 12, 151- 176.

Kung, E.C.,1966: Kinetic energy generation and dissipation in the large scale atmospheric circulation. Mon. Wea. Rev., 94, 67-82.

Michaelides, S. C., 1992: A spatial and temporal energetics analysis of a baroclinic disturbance in the Mediterranean. Mon. Wea. Rev., 120, 1224- 1243.

Michaelides, S. C., N.G. Prezerakos and E.Flocas, 1996: Lagrangian energetics of a Mediterranean depression. Proceedings of the 3rd Pan-Hellenic Conference on Meteorology, Climatology and Atmospheric Physics, Athens, Greece, 25- 27.

Mohanty, U. C., P. V. S. Raju and R. Bhatla .2006: A Study on Climatological Features of the Asian Summer Monsoon: Dynamics, Energetics and Variability. Pure and Applied Geophysics, 162, 1511- 1541.

O'Brien, J.J., 1970: Alternative solutions to the classical vertical velocity problem. J. Appl. Meteor., 9, 197- 203.

Pant. G. B, 2005:Energetics of open atmospheric systems: Case study of an extratropical cyclone. Meteorol. Atmos. Phys, 31,39-62.

Silas Chr Michaelides, 2006: Components of large-scale kinetic energy generation during an eastern Mediterranean cyclogenesis, Meteorol. Atmos. Phys. 32, 247- 256.

Smith, P. J., 1969: On the contribution of a limited area to the global energy budget. Tellus, 21, 202- 207.

Smith, P. J., 1973: The kinetic energy budget over north America during a period of major cyclone development. Tellus, 25, 411-423.

Tsing-Chang Chen and Yen-Huei Lee, 2004: A note on the maintenance of the atmospheric kinetic energy. Pure and Applied Geophysics, 120, 642- 647.

Tsui T. L., and E. C. Kung, 1977: Subsynoptics-Scale energy transformations in various sever storm situations. J. Atmos. Sci., 34, 98-110.

Uccellini, L. W., and D. R. Johnson, 1979: The coupling of upper and lower tropospheric jet streaks and implications for the development of severe convective storms. Mon. Wea. Rev., 107, 682- 703.

Wiin- Nielsen, 1968: On the intensity of the general circulation of the atmosphere. Rev, Geophys., 6, 559- 579.

Ward, J. H., and P. J. smith, 1976: A kinetic energy budget over North America during a period of short synoptic wave development. Mon. Wea. Rev., 104, 836- 848.

Yousef. A. S. 1988: Development and application of a limited area numerical model. Ph.D. Thesis. Cairo University 170pp.
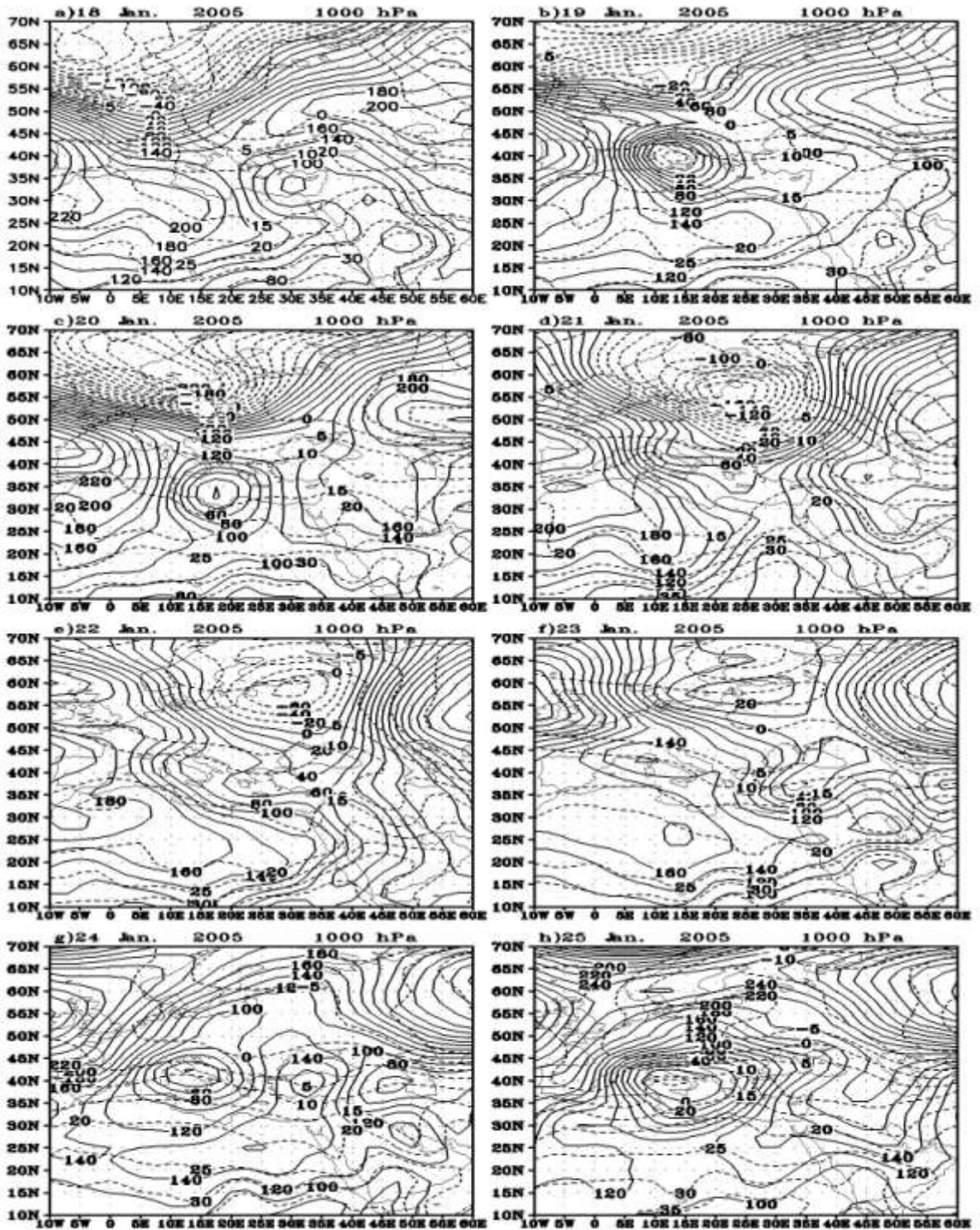
Fig. 1. 1000 hPa height contours in 20 m intervales (solid) and temperature (dotted) in 5°C increments for 1200 UTC 18- 25 January 2005.
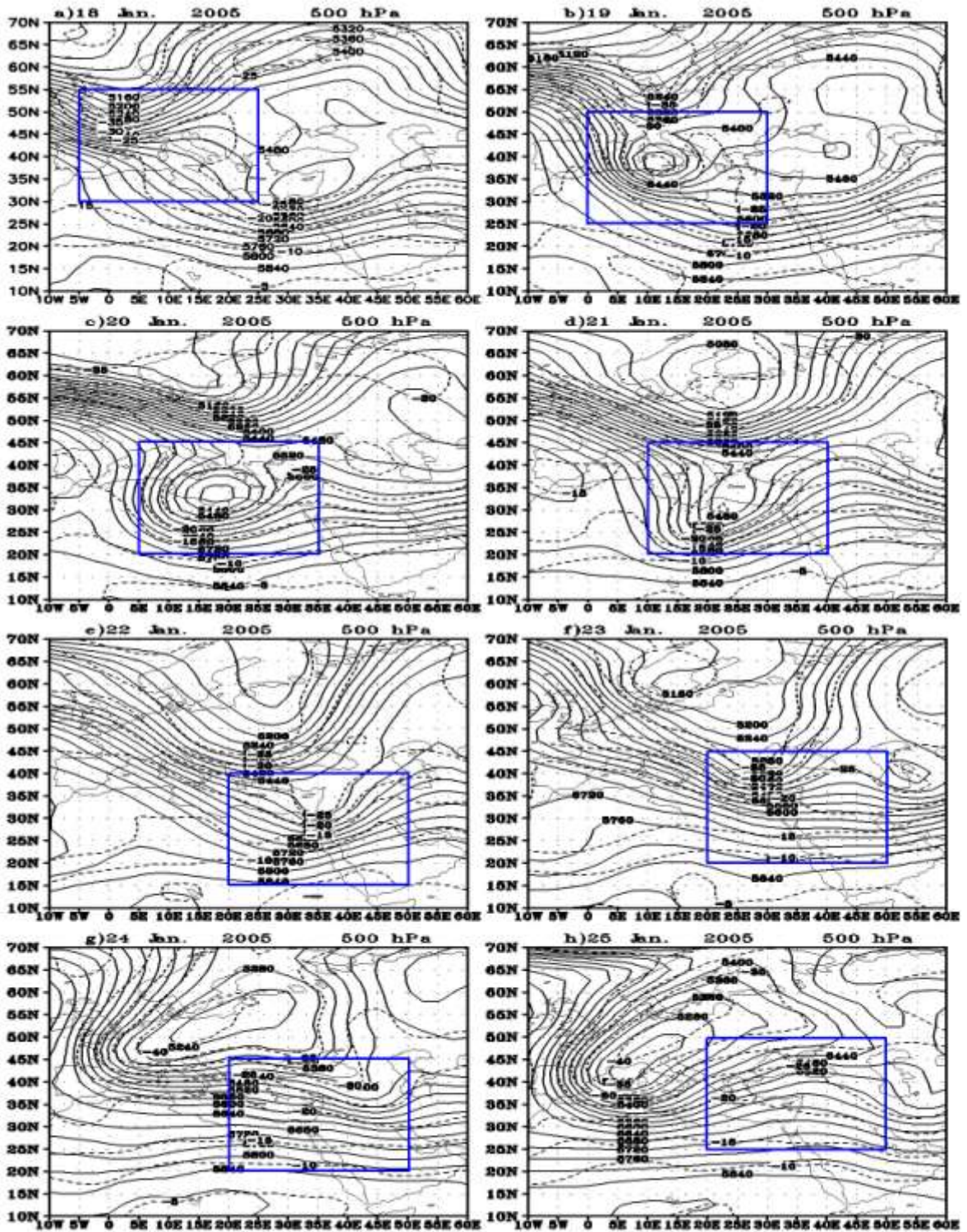
Fig. 2. 500 hPa height contours in 60 m intervales (solid) and temperature (dotted) in 5°C increments for 1200 UTC 18- 25 January 2005.
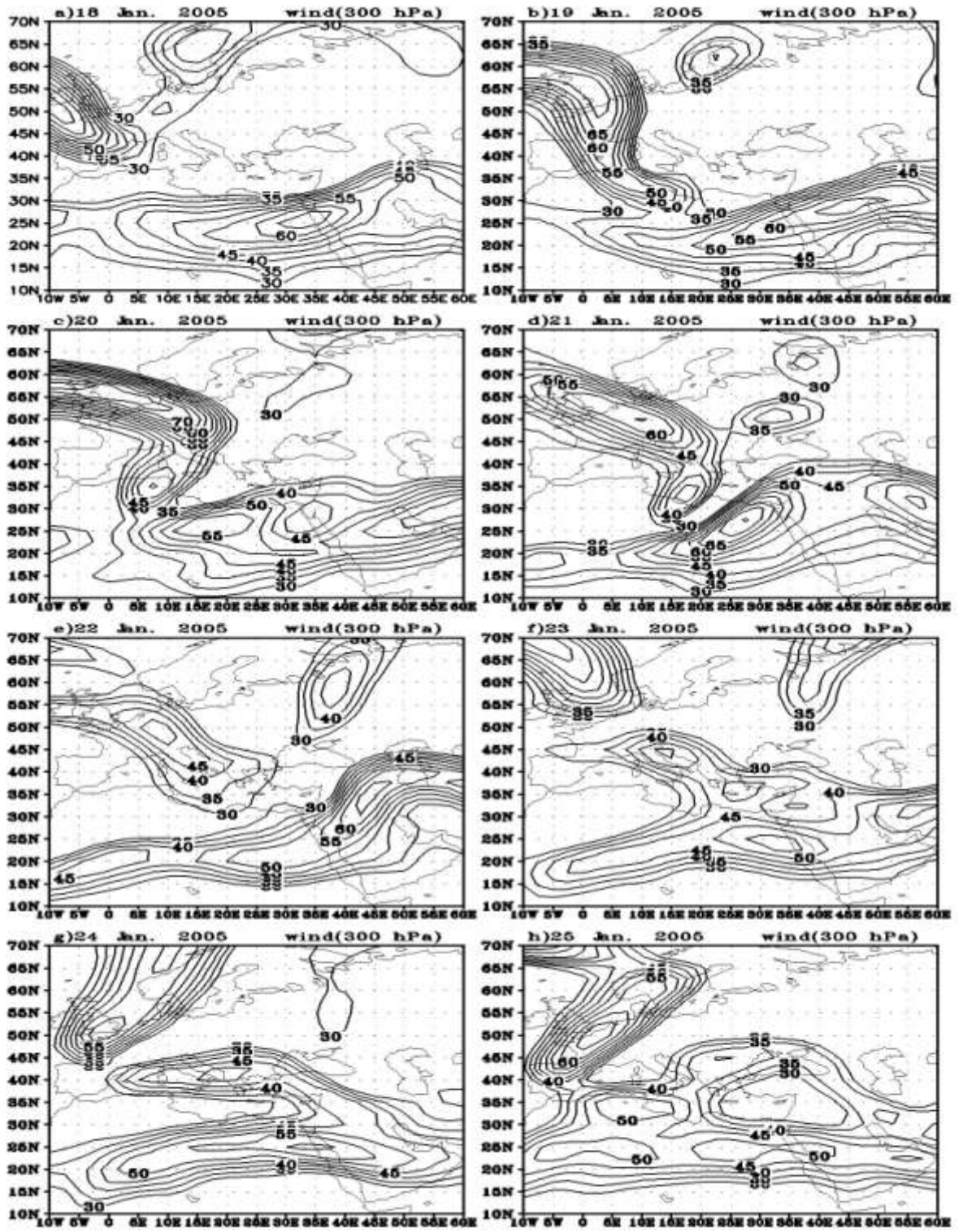
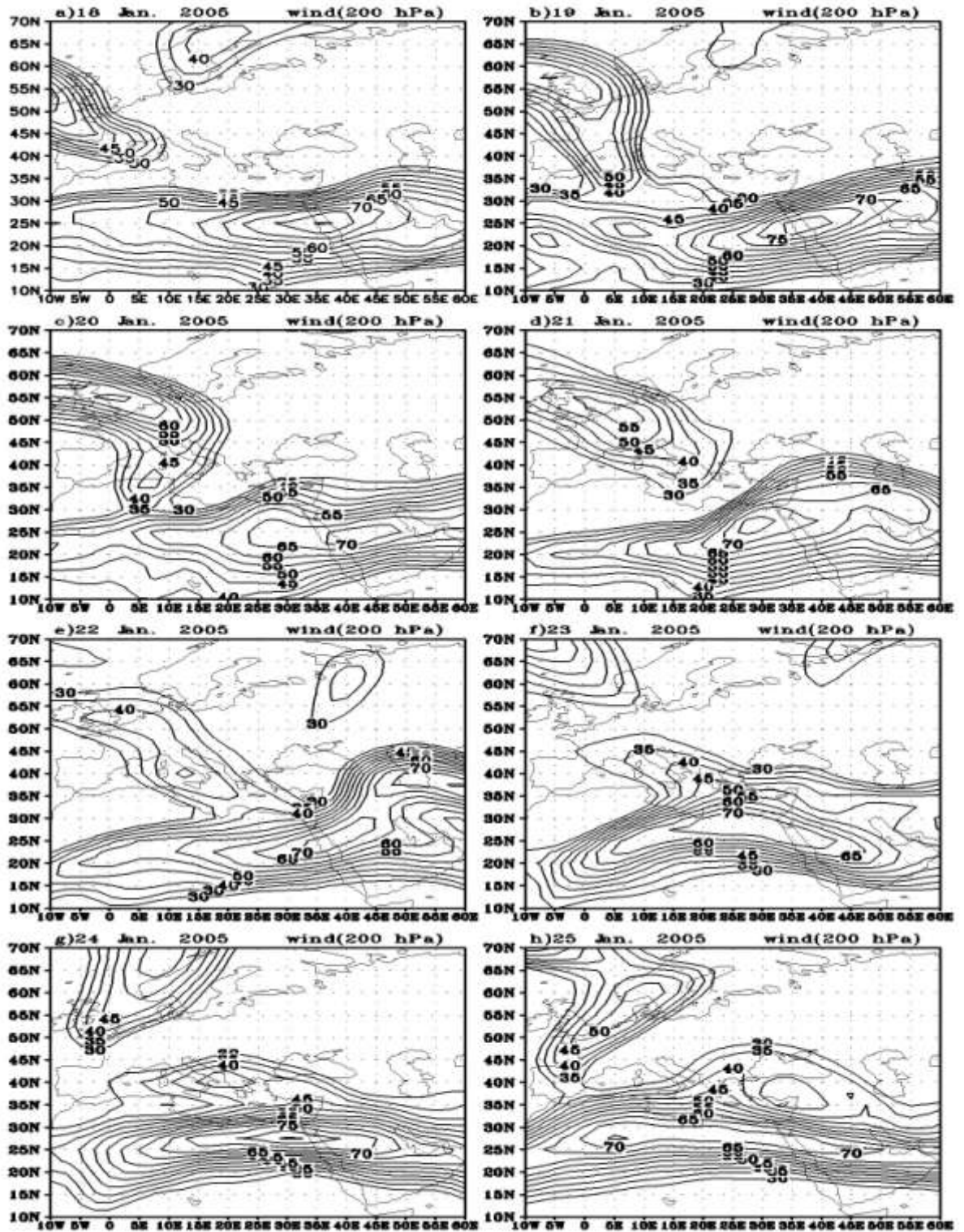Fig. 3. 300 hPa isotach (wind speed > 30 m/s) during the period 18- 25 January 2005.

Fig. 4. 200 hPa isotach (wind speed > 30 m/s) during the period 18- 25 January 2005.
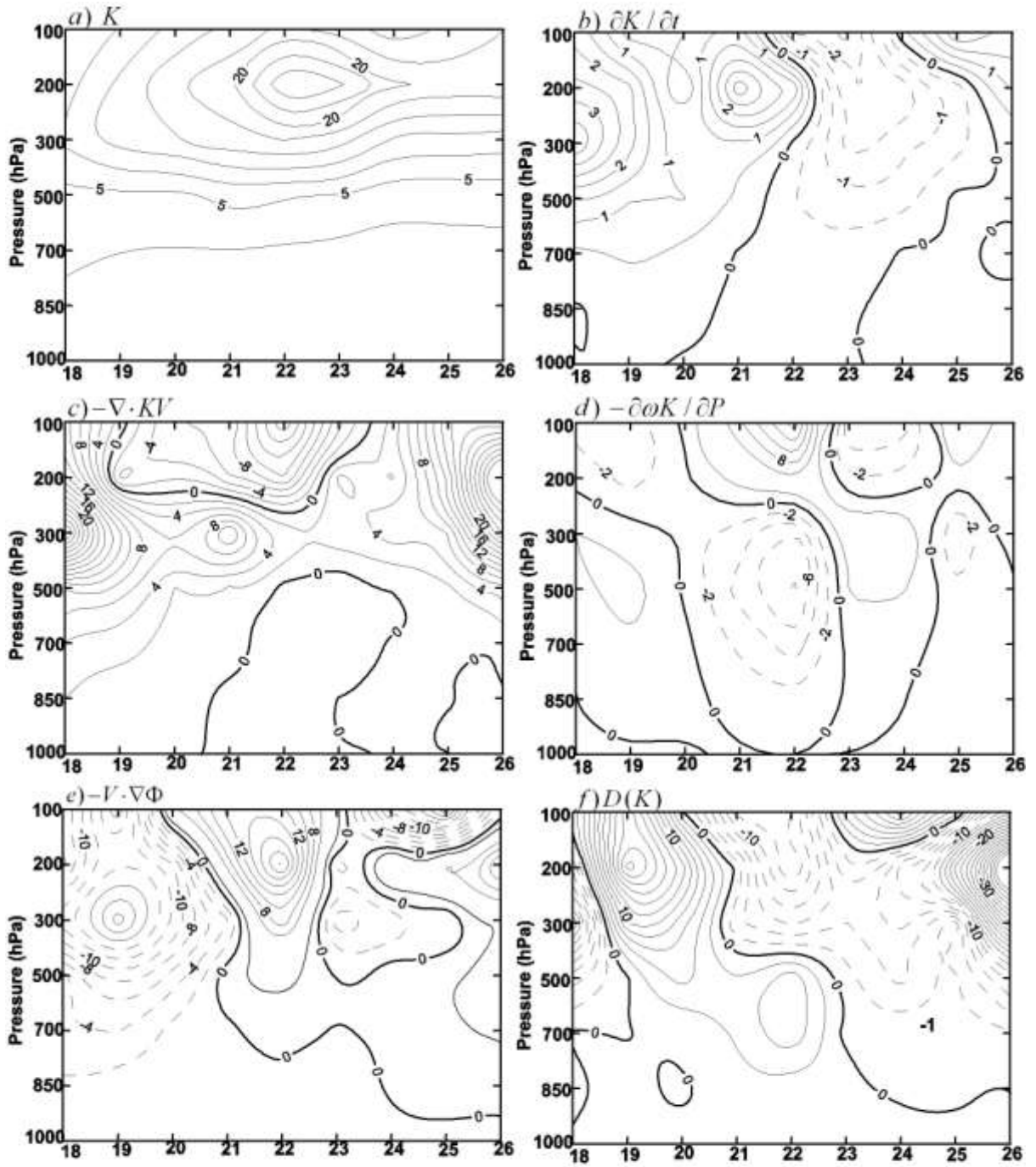
Fig. 5 : Pressure time cross sections of kinetic energy and kinetic energy budget terms.
Units: kinetic energy in 10^{-5} Jm^{2}(100 hPa)   .
kinetic energy changes in Wm^{2} (100 hPa)   .
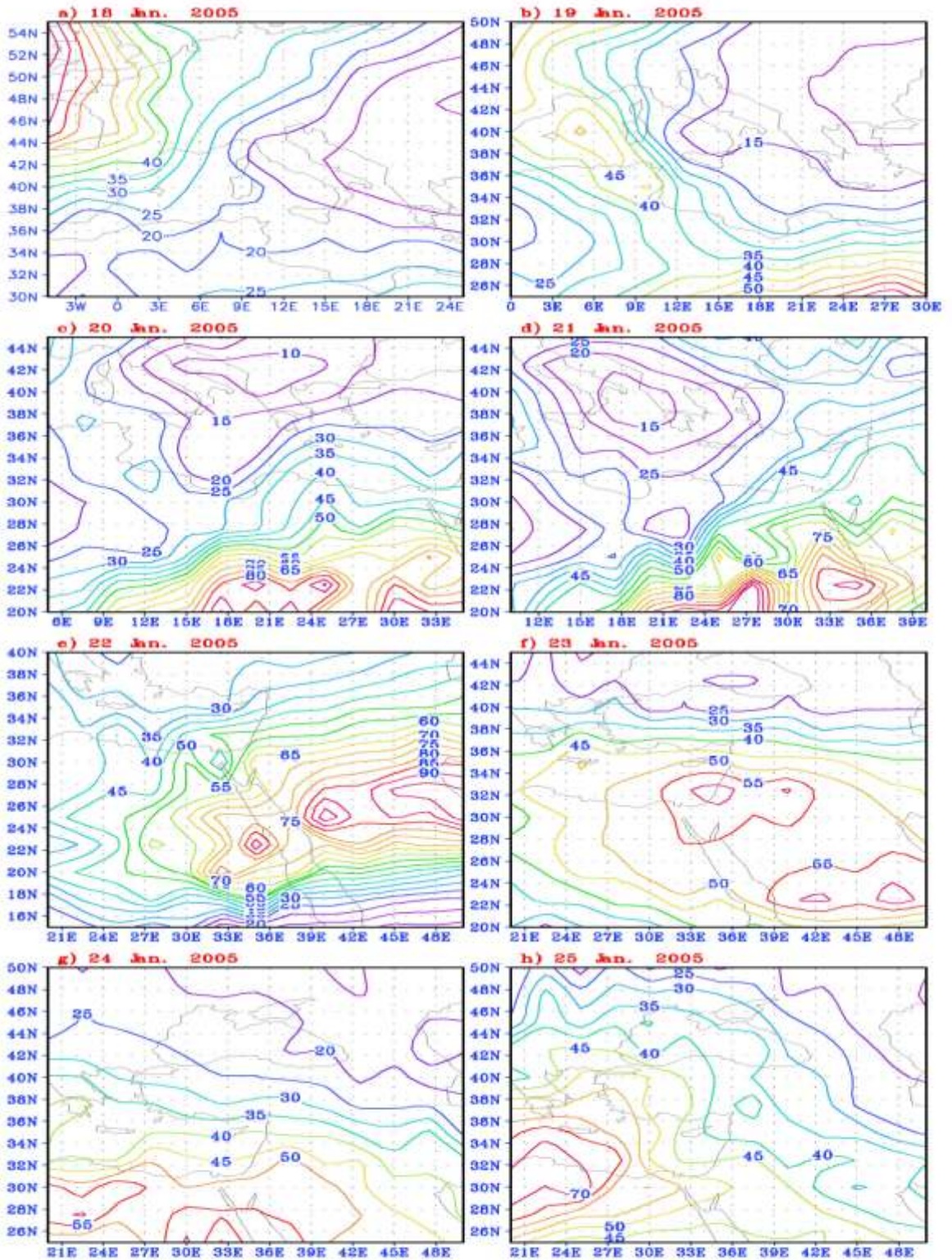
Fig. 6: Horizontal maps of kinetic energy content in the layer 200- 400 hPa for 1200 UTC 18- 25 January 2005. Units are $10^5 \, Jm^{-1}$.
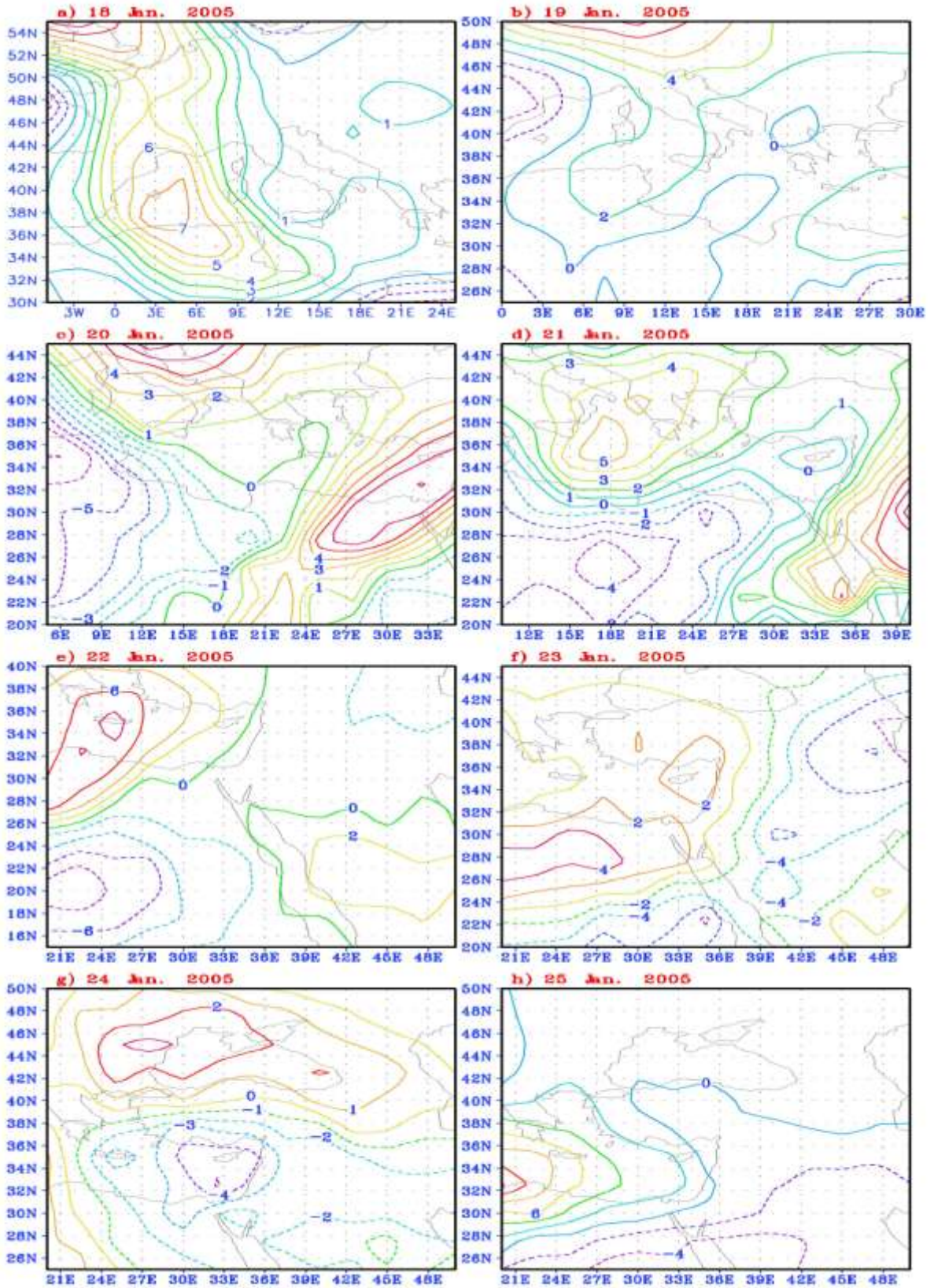
Fig. 7: Horizontal maps of $\partial K / \partial t$ (1000 - 100 integrated values) for 1200 UTC 18- 25 January 2005. Units are Wm^{2}.
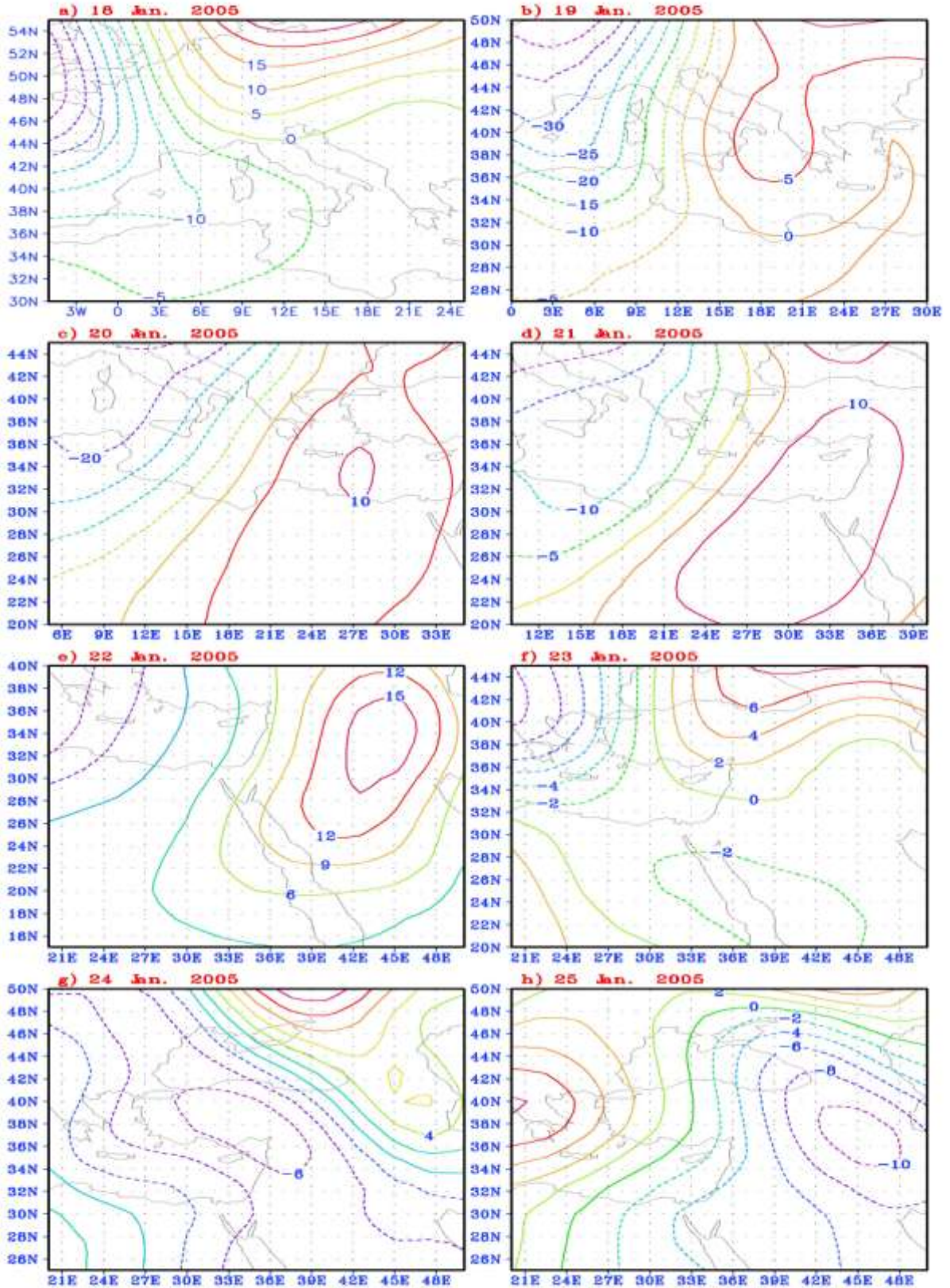
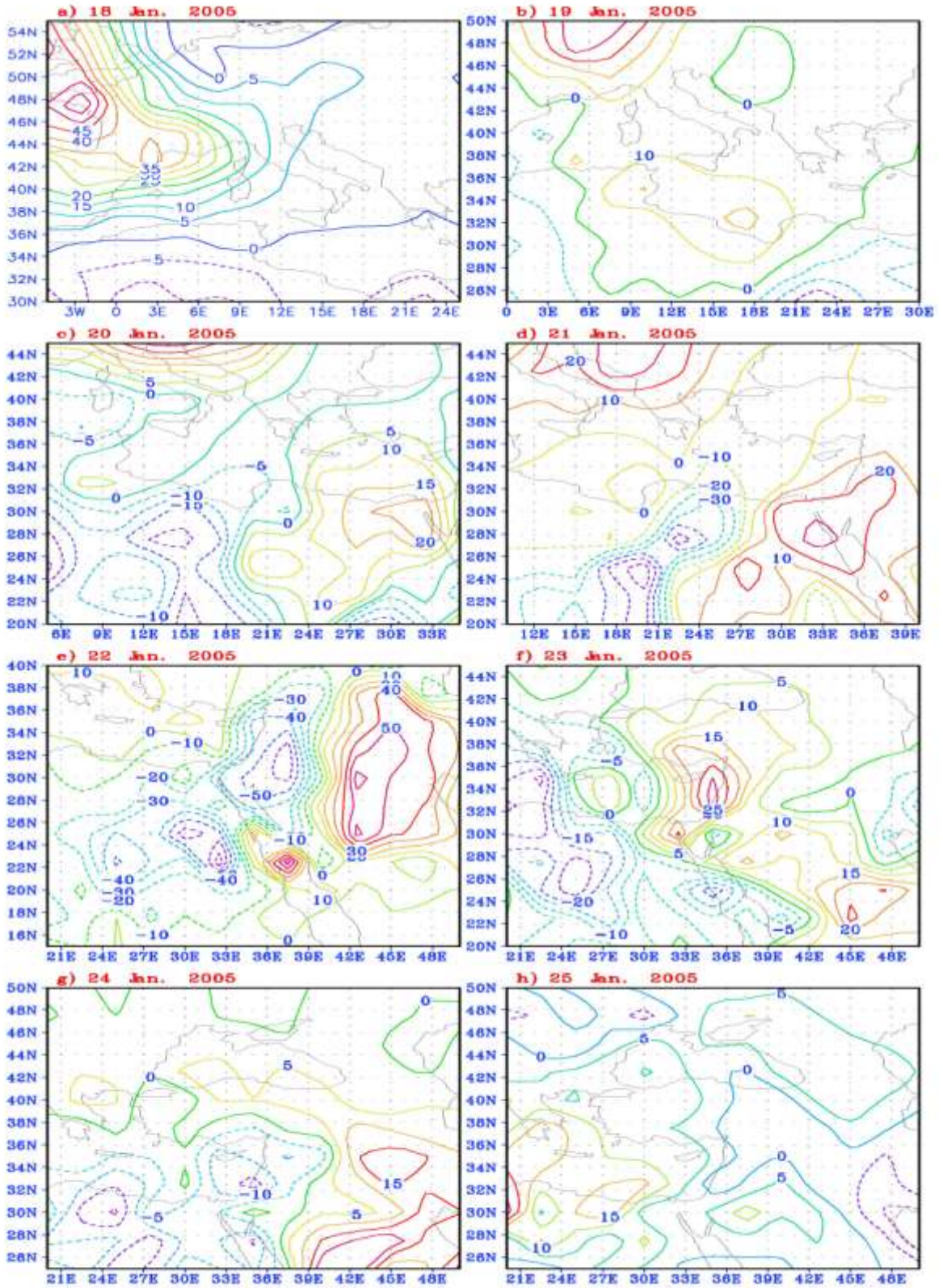Fig. 8: Horizontal maps of $-V \cdot \nabla \Phi$ (1000 - 100 integrated values) for 1200 UTC 18- 25 January 2005. Units are Wm^2.

Fig. 9: Horizontal maps of $-\nabla \cdot Vk$ (1000 - 100 integrated values) for 1200 UTC 18- 25 January 2005. Units are Wm^{-2}.
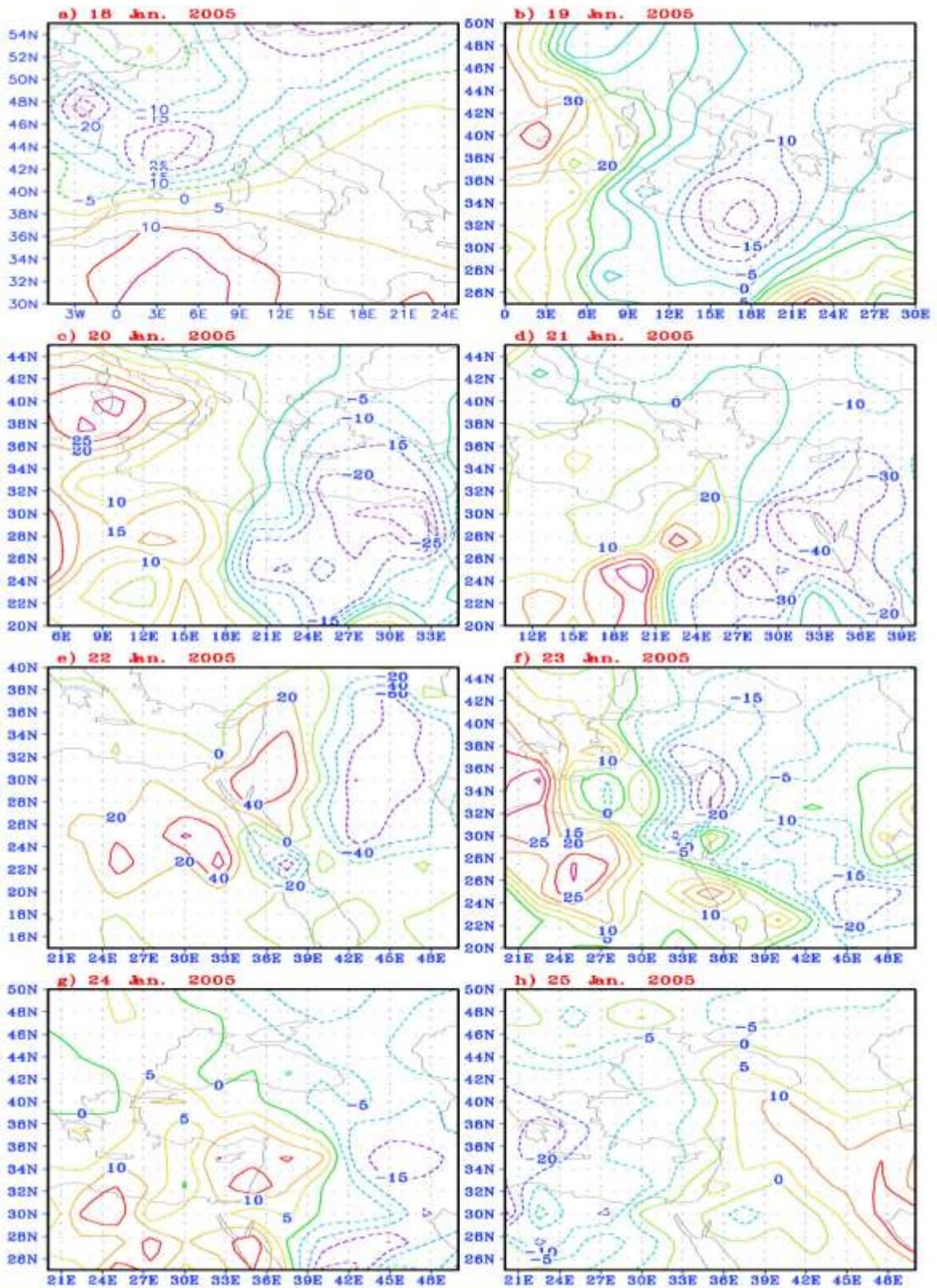
Fig. 10: Horizontal maps of D(K) (1000 - 100 integrated values) for 1200 UTC 18- 25 January 2005. Units are Wm^{-2}.